Gas-to-Particle Conversion in the Particle Precipitation–Aided Chemical Vapor Deposition Process II. Synthesis of the Perovskite Oxide Yttrium Chromite

V. E. J. van Dieten,* J. P. Dekker, E. J. Hurkmans, and J. Schoonman
Laboratory for Applied Inorganic Chemistry, Delft University of Technology, Julianalaan 136, 2628 BL Delft, The Netherlands

In the particle precipitation–aided chemical vapor deposition process, an aerosol is formed in the gas phase at elevated temperatures. The particles are deposited on a cooled substrate. Coherent layers with a controlled porosity can be obtained by a simultaneous heterogeneous reaction, which interconnects the deposited particles. The synthesis of submicrometer powder of the perovskite oxide yttrium chromite ($YCrO_3$) by gas to particle conversion, which is the first step of the PP-CVD process, has been investigated, and preliminary results are shown. The powders have been synthesized using yttrium trichloride vapor (YCl_3), chromium trichloride vapor ($CrCl_3$), and steam and oxygen as reactants. The influence of the input molar ratio of the elements on the composition and characteristics of the powders has been investigated. Phase composition has been determined by X-ray diffraction (XRD). The powders have been characterized by transmission electron microscopy (TEM) and sedimentation field flow fractionation (SF^3). At a reaction temperature of 1283 K the powders consist of chromium sesquioxide (Cr_2O_3), or a mixture of Cr_2O_3 and $YCrO_3$. At stoichiometric input amounts of metal chlorides and steam the formation of $YCrO_3$ seems to be favored. Two typical particle size distributions have been observed. The primary particle size ranges from 5 to 30 nm for small particles, and from 40 to 250 nm for large particles, depending on the process conditions. The particles tend to be agglomerated. The weight of the agglomerates is independent of the primary particle diameter.

INTRODUCTION

A solid oxide fuel cell (SOFC) is a device for the generation of direct-current electric power. An advantage fuel cells have over most conventional forms of power generation is that they are not Carnot limited. While many other modes of power generation involve thermodynamic inefficient conversion of heat to mechanical energy, fuel cells convert the free energy of a chemical reaction directly into electrical energy. Therefore, high fuel efficiency and potentially very large power density (W/kg) are possible (Hammou, 1992; Kinoshita et al., 1988).

A schematic representation of a SOFC is given in Figure 1. A SOFC consists of a gastight oxygen ion conducting solid electrolyte, a porous oxygen electrode (cathode), and a porous fuel electrode (anode). For cell operation, oxidant (air or oxygen) flows through the cathode, and fuel (e.g., hydrogen or carbon monoxide) flows through the anode. When an external load is applied the oxygen at the cathode reacts with the incoming electrons to

*To whom correspondence should be addressed.

0278-6826/93/$6.00
Aerosol Science and Technology 19:562–574 (1993)

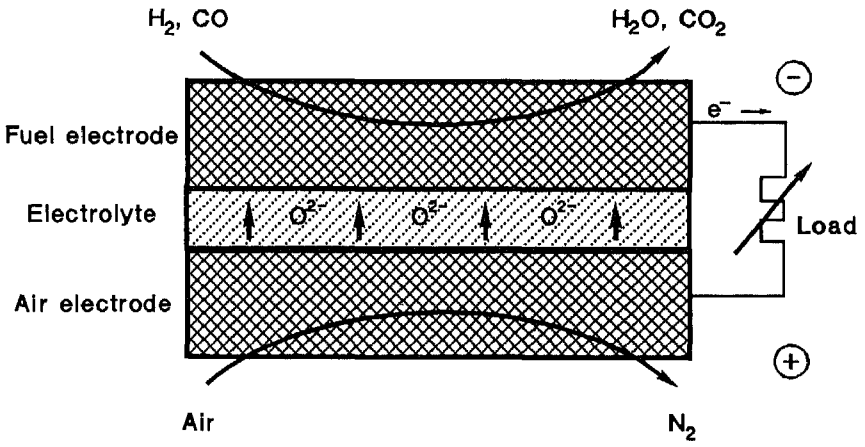

FIGURE 1. Schematic representation of the concept of a SOFC.

form oxygen ions. These oxygen ions diffuse through the oxygen ion conducting electrolyte to the anode, where they react with the fuel to form oxidation product and electrons, which are released into an external circuit. The solid electrolyte has to be gastight to prevent direct combustion of the fuel. The electrodes have to be porous in order to allow easy gas transport to the electrode–electrolyte interface. Charge transfer reactions take place at the ternary interface gas–electrode–electrolyte. SOFCs operate at high temperatures (> 800°C), which has a favorable effect on the reaction kinetics at the ternary interface and mass transfer through the electrolyte. The fast kinetics eliminate the necessity of using expensive noble metal catalysts.

The open circuit of the cell is given by the Nernst equation,

$$E = \frac{RT}{nF} \ln\left\{\frac{p_{O_2}(\text{cathode})}{p_{O_2}(\text{anode})}\right\} \qquad (1)$$

where R is the gas constant, T is the operating temperature (K), n is the number of electrons involved in the cell reaction, F is the Faraday constant, and p_{O_2} is the oxygen partial pressure in the gas at the cathode and the anode, respectively. At 1273 K, using air as oxidant and a fuel with an oxygen partial pressure of about 10^{-12} Pa, the open circuit voltage of a single cell is about 1 V (Singhal, 1991). To form a power generator, several elementary cells have to be connected parallel or in series, using an appropriate interconnection material. The interconnection material connects the anode of one cell with the cathode of the next. Therefore, it has to be gastight to prevent direct combustion of the fuel. Furthermore, the interconnection material has to be chemically stable in both oxidizing and reducing atmospheres.

A variety of configurations is now being considered for the SOFC. These include tubular, monolithic and planar concepts (Hammou, 1992). The research and development of SOFCs has led to the "state of the art" materials and fabrication techniques listed in Table 1 (Singhal, 1991). For the thin-film tubular SOFC configuration developed by Westinghouse the contribution of the individual components to the total cell resistance is given in Table 2 (Steele, 1990).

TABLE 1. "State of the Art" Materials and Fabrication Techniques for SOFC Components

Component	Material	Fabrication technique
Electrolyte	YSZ (8–10 mol%)	electrochemical vapor deposition, tape casting
Interconnect	$LaCr_{1-x}Mg_xO_3$	electrochemical vapor deposition, tape casting
Cathode	$La_{1-x}Sr_xMnO_3$	slurry coating, tape casting
Anode	Ni-YSZ cermet	slurry coating, tape casting

The materials used in a SOFC have to fulfil the following requirements:

1. Good chemical and mechanical stability at operating conditions;
2. High electrical conductivity of the individual components;

   Good mixed (electronic and ionic) conducting materials are preferred for the electrodes.

   Good electronic conductivity, with negligible ionic conductivity is required for the interconnection material.

   Good oxygen ion conductivity is required for the solid electrolyte.

3. Thermal expansion coefficients of the individual components should match.

Perovskite oxides ABO_3, containing a rare earth metal ion (3^+) on the A-site, and a transition metal ion (3^+) on the B-site, are the most promising materials for application as SOFC component (Hammou, 1990; Alcock et al., 1992), because their intrinsic physical properties match closely the above mentioned requirements. Furthermore, the properties can easily be changed by (partially) substituting the A or B ions by other metal ions. The state of the art materials used for the cathode and the interconnect are perovskite oxides, as can be seen in Table 1.

The performance of a SOFC can be improved by using materials with superior electrical properties or by minimizing the thickness of the cell components. Both methods will lead to a reduction of the ohmic polarization losses. In recent years there has been an increased interest in the use of thin film components in SOFC's.

Thin films of the interconnection material are produced by tape casting and subsequent sintering or electrochemical vapor deposition (Table 2). These processes require very high temperatures, because they both are limited by solid state mass transport. However, the other cell components may not be chemically stable at these high temperatures.

Another synthesis method for thin films is conventional chemical vapor deposition (CVD). This technique allows one to synthesize thin films of metal oxides at moderate temperatures. However, it is difficult to form pinhole-free layers on a porous substrate, therefore, this technique as such is not well suited for the production of the interconnection material.

TABLE 2. Contribution of the Individual Components of a Tubular SOFC to the Total Cell Resistance

Component	R (1273 K) (Ω cm)	Thickness (mm)	Contribution to cell resistance (%)
Electrolyte (YSZ)	10.0	0.04	9
Interconnect ($LaCr_{1-x}Mg_xO_3$)	0.5	0.04	1
Cathode ($La_{1-x}Sr_xMnO_3$)	0.013	0.07	65
Anode (Ni-YSZ cermet)	0.001	0.10	25

A modified form of conventional CVD is particle precipitation–aided CVD (PP-CVD). The principle of the process is discussed elsewhere (Dekker et al., 1993). PP-CVD might be a suitable technique for the synthesis of the interconnection material, because it has been shown that it is possible to control the porosity of the deposited layers, and that also dense layers can be formed (Dekker et al., 1993).

In theory this technique can be used to produce all components of a single SOFC. In that case only one synthesis technique is used. Hence, a complete SOFC can be formed within one production step by only altering the reaction conditions. This production method has the following advantages over the conventional way of producing a complete SOFC:

- Fewer temperature cycles during production; hence, less risk of mechanical failure of the components;
- If produced at operating temperature, the SOFC will be stress-free during operation;
- Thin film components are produced, so ohmic polarization losses will be minimal;
- No contamination of the interfaces between the components.

Because there are few reports on powder synthesis of perovskite oxides in the gas phase, we have started to investigate the possibility to synthesize a perovskite oxide aerosol by gas-to-particle conversion. This report will discuss the preliminary results of the powder synthesis of the perovskite oxide yttrium chromite ($YCrO_3$) from the gas phase under experimental conditions, which are expected to be typical for the formation of the perovskite by heterogeneous reaction, which is necessary for the PP-CVD of the interconnection material. $YCrO_3$ can be formed using yttrium trichloride (YCl_3), chromium trichloride ($CrCl_3$), and steam (H_2O) and/or oxygen (O_2), as precursors (Feduska et al., 1978).

$$YCl_{3(g)} + CrCl_{3(g)} + 3H_2O_{(g)} \rightarrow YCrO_{3(s)} + 6HCl_{(g)} \quad (2)$$

$$2YCl_{3(g)} + 2CrCl_{3(g)} + 3O_{2(g)} \rightarrow 2YCrO_{3(s)} + 6Cl_{2(g)} \quad (3)$$

For the formation of thin films of binary oxides by CVD, using the metal chlorides as reactants, oxidant vapors as H_2O, O_2, or a CO_2/H_2 mixture can be used (Blocher, 1982). For example, Funk et al. (1975) described the formation of alumina particles in the vapor phase, in the reaction temperature region from 873 to 1273 K, using $AlCl_3$ and H_2O as reactants. We believe that, in general, a reaction between metal chlorides and steam will result in powder formation. In order to form films of metal oxides, a CO_2/H_2 mixture is usually used (Funk et al., 1975; and Sipp et al., 1992a,b). This mixture produces a very low concentration of H_2O. This formation takes place at the CVD surface. Consequently, the reactive H_2O will react with the metal chloride at the surface, which will prevent the formation of the metal oxides by homogeneous reaction. Because oxygen is less reactive than steam it might be possible that oxidation of the metal halides with oxygen can only take place by heterogeneous reaction.

An indication whether the formation of a solid occurs by a heterogeneous or a homogeneous reaction can be obtained by evaluating the thermodynamic equilibrium constant for the formation reaction. Kato et al. (1981) have studied the relation between the equilibrium constant and powder formation, for nitrides, carbides,

and oxides. They observed the tendency that powder formation only occurs when the equilibrium constant is large. Comparison of the equilibrium constants for the formation of binary oxides according to reactions (2) and (3) reveals that the equilibrium constants of the reactions using steam as oxidant are always larger. Hence, it might be possible that, under certain experimental conditions, using a mixture of steam and oxygen, the $YCrO_3$ aerosol is formed by reaction (2), while simultaneously the formation of $YCrO_3$ by heterogeneous reaction (3) takes place.

$YCrO_3$ is chosen instead of $LaCrO_3$, which is commonly used as interconnection material in a SOFC (Table 1), for practical reasons, because it is easier to obtain the necessary high gas phase concentrations of YCl_3 than of $LaCl_3$, because $LaCl_3$ is much less volatile than YCl_3. $YCrO_3$ is isostructural with $LaCrO_3$ and has almost the same electrical and thermal properties as $LaCrO_3$ (Carini et al., 1991).

$YCrO_3$ powder has been precipitated on a cooled quartz tube. The influence of the input molar ratio of the elements on the composition of the powder has been investigated.

EXPERIMENTAL ASPECTS

A schematic representation of the PP-CVD reactor is given in Figure 2. A conventional gas distribution system, as described by Dekker et al. (1993), is used. The reactor consists of a quartz tube (inner diameter 42 mm, and length 800 mm) in a two-zone resistance furnace (zone length 300 mm). The powders formed are collected on a cooled susceptor. The susceptor consists of a dead-end hollow quartz tube. The cooling of the susceptor is regulated by an externally controlled flow of pressurized air. The tip of the susceptor is positioned in the centre of the reactor tube, in the middle of the left heating zone. The metal chloride evaporator consists of a quartz tube (inner diameter 22 mm, and length 450 mm). Inside this tube there is a row of quartz containers for the solid metal trichlorides. The axial position of the evaporator can be

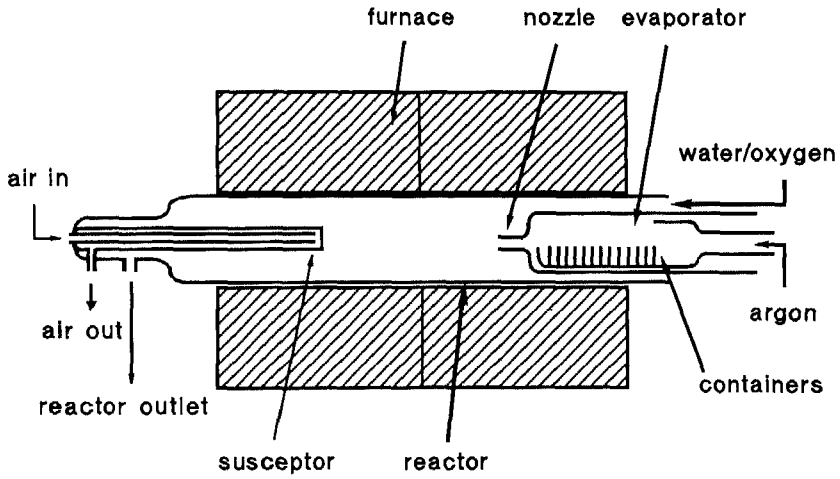

FIGURE 2. Schematic representation of the PP-CVD reactor for the synthesis of perovskite oxides.

varied. Argon (Ar) is used as carrier gas to transport the metal chloride vapors into the reactor. It is assumed that the gas phase concentration of the metal chlorides is determined by their vapor pressures at the evaporation temperature. By altering the place of the reactants in the reactor, their evaporation temperatures can be changed, owing to the axial temperature gradient in the reactor. Hence, the ratio of the concentration of metal chlorides in the gas phase can be controlled by varying the respective evaporation temperatures. The nozzle has an inner diameter of 4 mm. High linear gas velocities in the nozzle are used to prevent diffusion of steam and oxygen into the evaporator, avoiding oxidation of the solid metal chlorides. A mixture of Ar/H_2O or O_2/H_2O is fed into the reactor, on the outside of the metal chloride evaporator. Temperatures are measured with chromel-alumel thermocouples. The reaction temperature is measured at the outlet of the nozzle, where the reactants are in direct contact. Also, the temperatures of the solid metal chlorides, the temperature of the gas phase at the tip of the susceptor, at about 10 mm above the tip, as well as the temperature at the tip within the susceptor, are monitored.

In all experiments the reactor pressure was 1×10^4 Pa. Because of the low vapor pressures of the $CrCl_3$ and YCl_3, a low reactor pressure was used in order to obtain high concentrations of the metal chlorides. The reaction temperature was kept constant at about 1283 K. The temperature in the reactor at the tip of the susceptor was about 1333 K. The temperature at the quartz tip within the susceptor varied between 1013 K and 1161 K. The experimental conditions are summarized in Table 3.

The phase composition of the powders collected on the susceptor is determined by X-ray diffraction (XRD) (Philips PW 1840, CuKα). Particle sizes are obtained using transmission electron microscopy (TEM) (Philips EM 400) and sedimentation field flow fractionation (SF^3) (Du Pont). The performance of this SF^3 apparatus is described by Scarlett et al. (1991).

For TEM analysis part of the collected powder is suspended in methanol, and a TEM grid is dipped into the suspension. For SF^3 analysis part of the collected powder is suspended in an aqueous solu-

TABLE 3. Process Parameters for the Synthesis of $YCrO_3$ by PP-CVD

Temperature of gas phase at the tip of the susceptor		1333 K	
Temperature in the susceptor		1013–1161 K	
Temperature of gas phase at the outlet of the nozzle		1283 K	
Reactant flows outside metal chloride evaporator		without O_2	with O_2
	H_2O flow	8 or 16	0.61–3.82 μmol/s
	O_2 flow	0	48 μmol/s
	Ar flow	0.031–1.8	1.86 mmol/s
Reactant flows inside metal chloride evaporator	$CrCl_3$ flow	0.18–2.01	0.22–1.43 μmol/s
	YCl_3 flow	0.17–1.33	0.32–1.27 μmol/s
	Ar flow	19–93	19–37 μmol/s
	Cr/Y ratio	1–1.75	0.23–1.6
Reactor pressure		1×10^4 Pa	
Reaction time		5400–10,800 s	

tion of 0.1 vol% dioctyl sodium sulfosuccinate. The powder concentration in the suspensions was about 1.5 weight%.

RESULTS AND DISCUSSION

During the syntheses using only steam, a light green powder was collected on the cooled susceptor. During the experiments with a mixture of steam and oxygen, in most cases, light green powder was collected on the part of the susceptor within the furnace, whereas on the part of the susceptor outside the furnace the collected powder was dark green. In some experiments however, only light green powder was collected on the part of the susceptor within the furnace, whereas on the part of the susceptor outside the furnace no powder was collected. No clear relation is observed between process conditions and appearance of a powder deposit outside the furnace. In principle, the difference between the color of the particles collected inside, and outside the furnace may be caused by a difference in composition or particle size.

In experiments where only oxygen, and no steam, was present no powder was formed, but only deposition on the reactor wall, by a heterogeneous reaction, could be observed. This indicates that the reactivity of the gas mixture without steam is not high enough to induce nucleation in the gas phase, and that oxygen may be a suitable reactant for heterogeneous CVD of $YCrO_3$. Hence, for powder formation the presence of steam is necessary.

Two XRD patterns, typical for the powders collected, are shown in Figure 3. For comparison, the XRD patterns of single phase chromium sesquioxide (Cr_2O_3), yttria (Y_2O_3), and $YCrO_3$ are shown as well. The $YCrO_3$ powder used as reference was made by a solid state reaction between equimolar amounts of Cr_2O_3 and Y_2O_3, at 1548 K during 63 hours, according to the method of Strakhov and Novikov (1975). In Figure 4 XRD patterns of two powders, synthesized in the same experiment, collected inside and outside the furnace respectively, are shown. In all experiments where powder was collected inside, as well as outside the furnace, the powders were single-phase Cr_2O_3, as determined by XRD analysis. Because the amount of powder harvested is very small, the signal to background ratio in the XRD patterns is poor. Therefore, line-broadening XRD analysis, to obtain quantitative values for the primary particle size is not possible.

Comparison of the XRD patterns of the powders collected inside and outside the furnace (Figure 4) reveals that there is no difference in phase composition. The diffraction peaks in the XRD pattern of the powder collected outside the furnace are broad in comparison with those of the powder collected inside the furnace. This might be caused by a difference in particle size, indicating that the particle size of the powder collected outside the furnace is smaller than that of the powder collected inside the furnace. Furthermore, small particles appear to be dark, which may be caused by a more diffuse light scattering. From TEM analysis it could be concluded that the powder collected outside the furnace has a smaller particle size than the powder collected inside the furnace. This is in agreement with the results of the XRD analysis. Hence, the dark color of the small particles is caused by a more diffuse light scattering, and not by a different phase composition.

The possible difference in particle size could be explained by the difference in residence time in the hot reaction zone. The residence time in the hot reaction zone for the particles collected outside the furnace is on the order of 10^{-1} to 1 s, which is determined by the linear gas velocity in the reactor, whereas for the particles collected inside the furnace this residence time is on the order of 10^{3} to 10^{4}

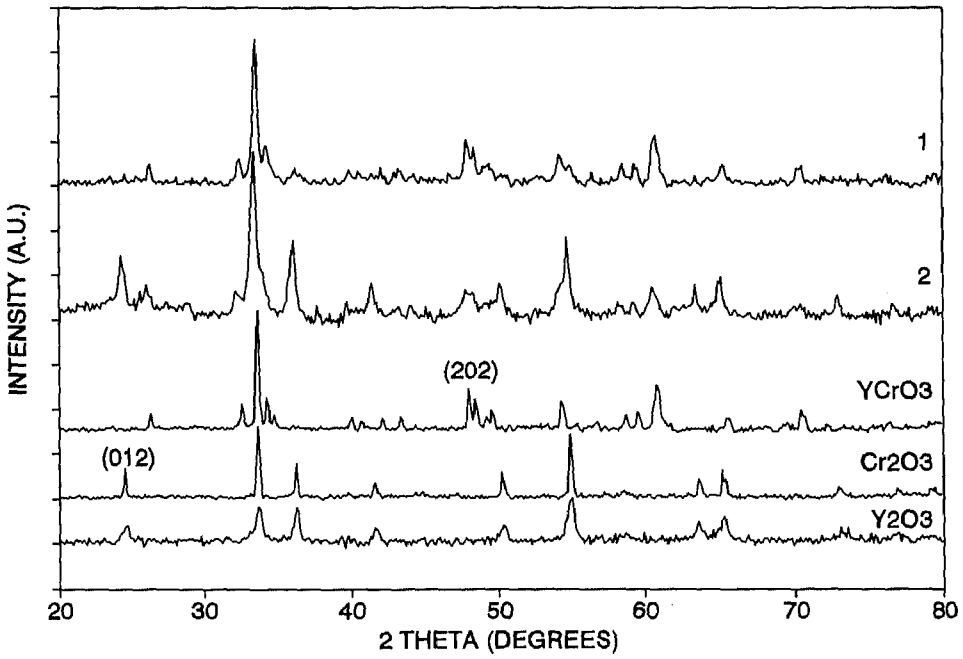

FIGURE 3. XRD patterns of powders synthesized by PP-CVD. For comparison the XRD patterns of Cr_2O_3, Y_2O_3, and $YCrO_3$ are shown as well. Synthesis conditions:

Powder 1	Powder 2
$\phi_{H_2O} = 2.43$ μmol/s	$\phi_{H_2O} = 2.48$ μmol/s
$\phi_{O_2} = 48.4$ μmol/s	$\phi_{O_2} = 48.4$ μmol/s
$\phi_{CrCl_3} = 0.69$ μmol/s	$\phi_{CrCl_3} = 0.65$ μmol/s
$\phi_{YCl_3} = 0.49$ μmol/s	$\phi_{YCl_3} = 1.00$ μmol/s

s, which is determined by the total process time. Hence, the particle size of the particles inside the furnace could increase, due to sintering, or heterogeneous reaction, whereas outside the furnace the temperature is too low for these processes to occur.

From the XRD patterns it can be seen that always Cr_2O_3 (Figure 4) or a mixture of Cr_2O_3 and $YCrO_3$ is formed (Figure 3). Only in a few cases Y_2O_3 could be identified.

For the different experiments various amounts of $YCrO_3$ with respect to Cr_2O_3 have been observed. In principle, there are several parameters which may affect the total amount of $YCrO_3$ formed. Besides reaction temperature, the input molar ratios of the elements determine which solid product will be formed. In our experiments the input molar ratios have been chosen such that a broad range of ratios were covered, e.g., $0.18 < Cr/(Cr + Y) < 0.60$.

In order to obtain semi-quantitative values for the ratio of the amount of $YCrO_3$ over Cr_2O_3 present in the collected powders, the ratio of the intensity of the $YCrO_3$ (202) reflection ($2\theta = 47.800°$, relative intensity = 24%) over the Cr_2O_3 (012) reflection ($2\theta = 24.483°$, relative intensity = 75%) is calculated from the XRD patterns (Figure 3). The strongest reflections of both Cr_2O_3 (104)

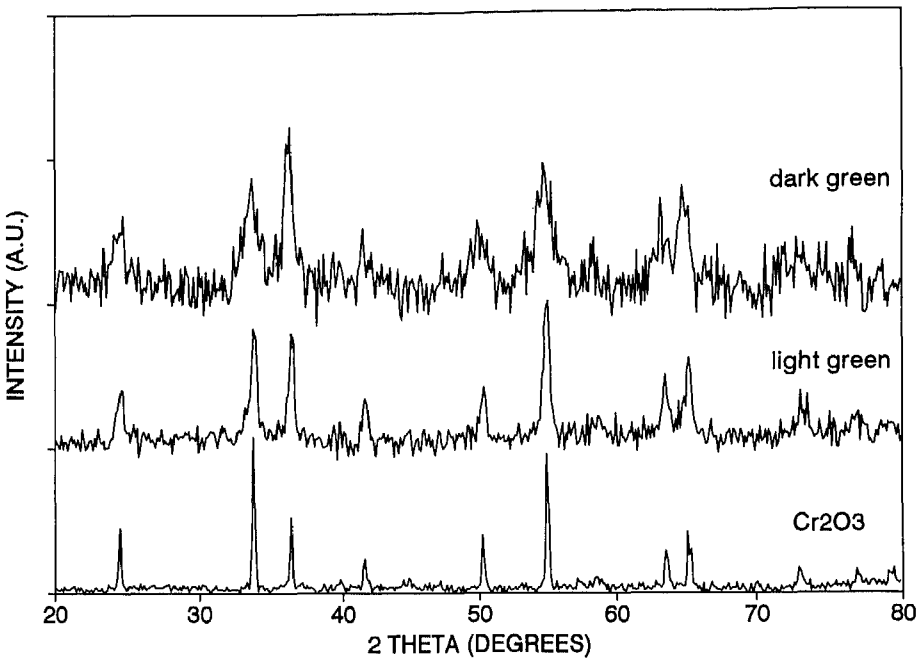

FIGURE 4. XRD patterns of a light, and dark green powder from one experiment. For comparison the XRD pattern of Cr_2O_3 is shown as well. Synthesis conditions: $\phi_{H_2O} = 2.84$ μmol/s, $\phi_{O_2} = 48.4$ μmol/s, $\phi_{CrCl_3} = 1.43$ μmol/s, and $\phi_{YCl_3} = 0.92$ μmol/s.

and $YCrO_3$ (121) could not be used, because these reflections do overlap.

Figure 5 shows the ratio $I_{YCrO_3\,(202)}/(I_{YCrO_3\,(202)} + I_{Cr_2O_3\,(012)})$ as a function of the ratio of the input concentrations of the metal chlorides. The input amount of water and metal chlorides was stoichiometric with respect to the desired perovskite oxide product. From this figure it can be seen that there is a maximum in the relative amount of $YCrO_3$ formed, with respect to Cr_2O_3, at a $CrCl_3/(CrCl_3 + YCl_3)$ ratio of 0.4. Hence, the tendency is that near stoichiometric input amounts of the elements, i.e., $Cr:Y:O_{from\ H_2O}:H = 1:1:3:6$, the formation of $YCrO_3$ is favored mostly.

In general, at the reaction conditions chosen, the formation of the binary oxide Cr_2O_3 is favored over the formation of $YCrO_3$ and Y_2O_3. This could be caused by either kinetic or thermodynamic limitations. Thermodynamic equilibrium calculations may elucidate this problem. These calculations can be performed using the SOLGASMIX program by Eriksson (1975), or the Chemsage program by Eriksson and Hack (1991). These programs minimize the free Gibbs energy of a system, considering all species. In case of thermodynamic limitations, experimental conditions have to be chosen such that $YCrO_3$ is the only stable solid species. In case of kinetic limitations, it is possible that, although according to thermodynamic equilibrium calculations only one solid phase is stable, e.g., $YCrO_3$, other solid phases, e.g., Cr_2O_3, are formed. The most obvious reaction parameter to change is the reaction temperature. Prob-

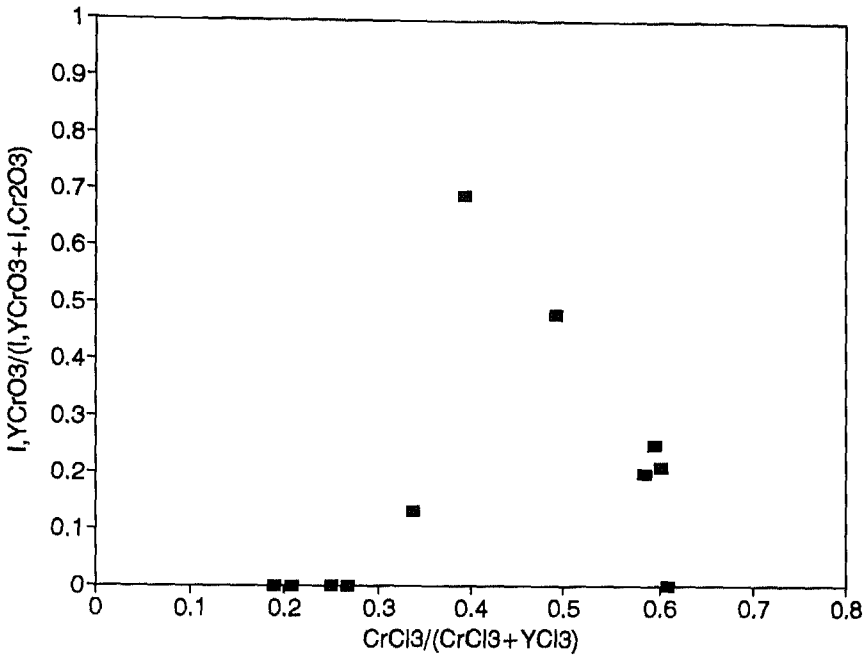

FIGURE 5. The ratio of the $YCrO_3$ (202) and Cr_2O_3 (012) reflections as a function of the fraction of $CrCl_3$ in the total metal chloride flux.

ably higher reaction temperatures are needed to form single phase $YCrO_3$, because thermodynamic calculations in the strongly related system La-Cr-O-H-Cl-Ar reveal that at relative low reaction temperatures (< 1573 K) both $LaCrO_3$ and Cr_2O_3 are stable, whereas at high reaction temperatures (> 1573 K) $LaCrO_3$ is the only stable solid phase (Van Dieten and Schoonman, 1993).

Figure 6 shows TEM micrographs of some typical examples of collected powders. The TEM micrographs reveal that the particles are agglomerated. From these micrographs it is not clear whether agglomeration is caused by evaporation of the liquid phase (methanol) during TEM sample preparation, or is a result of synthesis conditions.

In some experiments (Figure 6c), two different primary particle sizes could be determined in one micrograph. This bimodal particle size distribution is typical for the initial stage of the gas to particle conversion (Okuyama, 1986), assuming simultaneous chemical reaction and agglomeration of the particles in the gas phase.

There is no relation between the primary particle size, determined from the TEM micrographs (d_{TEM}), and the ratio of the concentration of metal chlorides, or the total metal chloride flux at constant reactor pressure, i.e., the total metal chloride concentration. The size of the small particles ranges from 5 to 30 nm, whereas the size of the larger particles ranges from 40 to 250 nm.

The mass mean diameter, as determined by SF^3 measurements (d_{SF^3}), is independent of the process conditions, and varies between 140 and 190 nm. This mass mean diameter differs significantly from the primary particle diameter, as deter-

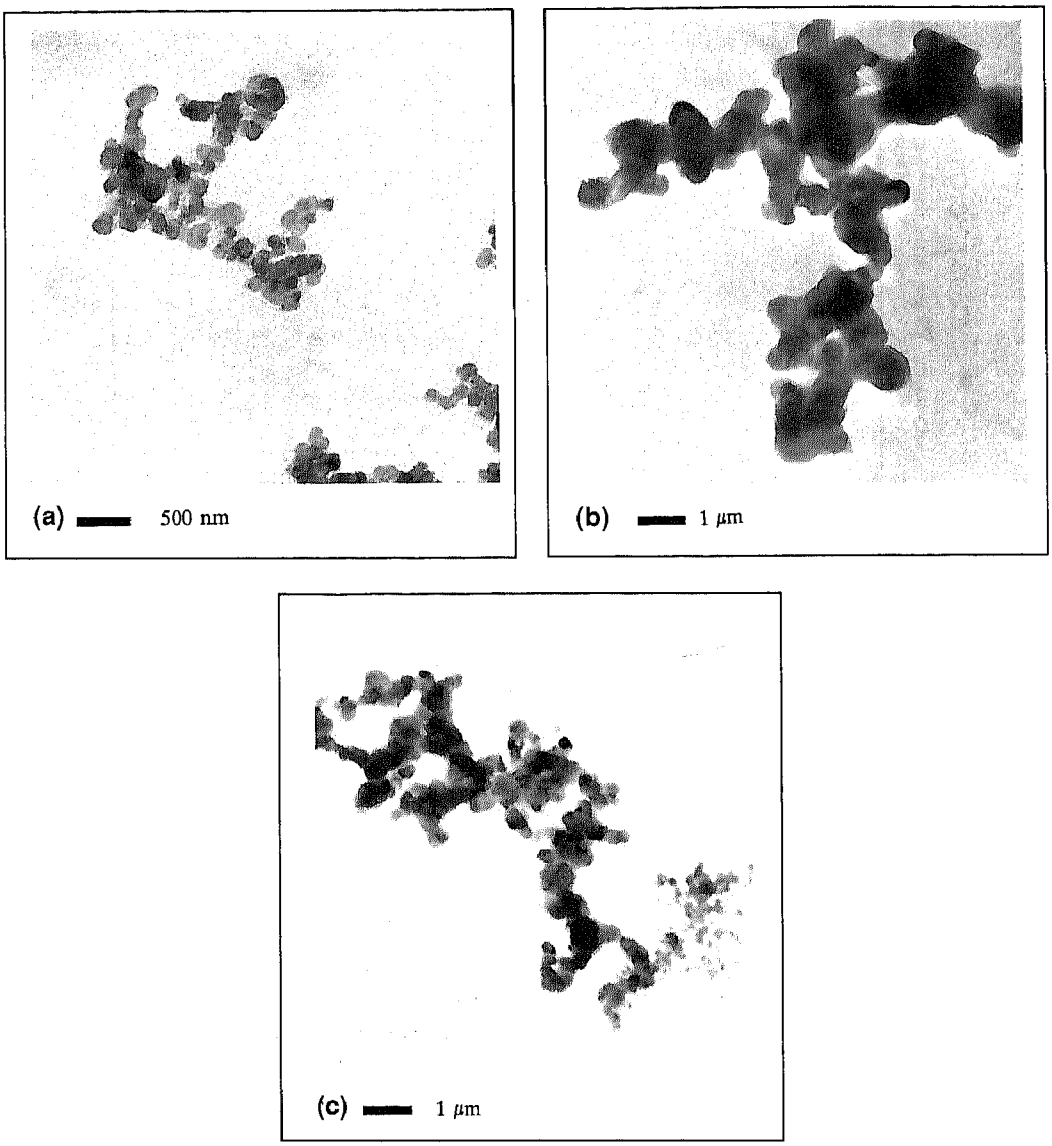

FIGURE 6. TEM micrographs of powders precipitated at different conditions. (a) $\phi_{H_2O} = 2.84$ μmol/s, $\phi_{O_2} = 48.4$ μmol/s, $\phi_{CrCl_3} = 0.25$ μmol/s, $\phi_{YCl_3} = 0.95$ μmol/s; (b) $\phi_{H_2O} = 2.42$ μmol/s, $\phi_{O_2} = 48.4$ μmol/s, $\phi_{CrCl_3} = 0.32$ μmol/s, $\phi_{YCl_3} = 0.33$ μmol/s; (c) $\phi_{H_2O} = 8.00$ μmol/s, $\phi_{CrCl_3} = 0.91$ μmol/s, $\phi_{YCl_3} = 0.62$ μmol/s.

mined from TEM micrographs (d_{TEM}). Hence, it can be concluded that the particles are agglomerated. Whether agglomeration is a result of the experimental conditions can be determined by comparison of d_{SF^3} with an equivalent mass diameter, determined from TEM micrographs. This equivalent mass diameter can be obtained by counting the number of primary particles in the agglomerates. By multiplying this number by the mass of the primary particles, the weight of the agglomerates is obtained, assuming that the primary particles are fully dense. The weight of the agglomerates, determined in this way, should fall within the mass distribution, obtained by SF^3 analysis. The number of primary particles in the agglomerates, as determined by counting, is typical on the order of 100–500, for the small particles. The number of primary particles in the agglomerates consisting of large particles is less, i.e., on the order of 30 to 80. This seems to be consistent with the results of the SF^3 analysis, which revealed that the weight of the agglomerates is independent of the primary particle diameter. The average weight of the agglomerates, determined from TEM micrographs, results in an equivalent mass diameter of about 150 nm. This value is in agreement with the results of the SF^3 analysis. So it can be concluded that agglomeration did occur during the synthesis process. Hence, the appearance of agglomerates in the TEM micrographs is not a result of sample preparation.

CONCLUSIONS

It is possible to synthesize the perovskite oxide $YCrO_3$ from the gas phase, using metal chlorides, and steam and oxygen as precursors. At the reaction conditions chosen, Cr_2O_3, or mixtures of Cr_2O_3 and $YCrO_3$ are formed. Formation of single-phase $YCrO_3$ is inhibited by either thermodynamic or kinetic limitations. Thermodynamic equilibrium calculations could elucidate this problem. In combination with these calculations, further experiments need to be performed in order to determine the range of reaction conditions, in which single phase $YCrO_3$ powder is formed. Especially higher reaction temperatures need to be considered.

If these reaction conditions are known, it is useful to determine the conditions for the heterogeneous formation of $YCrO_3$ in separate experiments, using experimental conditions within the range necessary for the homogeneous reaction to take place.

Then, it might be possible to choose reaction conditions such that the homogeneous and heterogeneous reactions occur simultaneously, which is a necessity in the PP-CVD process, for the formation of films of perovskite oxides with controlled morphology.

REFERENCES

Alcock, C. B., Doshi, R. C., and Shen, Y. (1992). *Solid State Ionics* 51:281.

Blocher Jr., J. M. (1982). In *Deposition Technologies for Films and Coatings* (R. Bunshah, ed.). Plenum, New York, p. 335.

Carini II, G. F., Anderson, H. U., Sparlin, D. M., and Nasrallah, M. M. (1991). *Solid State Ionics* 49:233.

Dekker, J. P., Put, P. J. van der, Veringa, H. J., and Schoonman, J. (1993). *Aerosol Sci. Technol.* 19:549–561.

Dieten, V. E. J. van, and Schoonman, J. (1993). To be presented at *184th Meeting of The Electrochemical Society,* New Orleans, October 10–15 1993.

Eriksson, G. (1975). *Chem. Scripta* 8:100.

Eriksson, G., and Hack, K. (1991). *Chemsage (Computer program).* GTT mbH, Aachen. Edition 2.1.1.

Feduska, W. and Isenberg, A. O. (1978). DOE Report CONS/1197-9 (Contract No. EY-76-C-03-1179), Westinghouse Electric Corporation, Pittsburgh, p. 48.

Funk, R., Schachner, H., Triquet, C., Kornmann, M., and Lux, B. (1975). In *Proceedings 5th International Conference on CVD* (J. Blocher, et al., eds.). The Electrochemical Society, Pennington, NJ, p. 469.

Hammou, A. (1992). In *Adv. Electrochem. Sci. Eng.* 2:88.

Kato, A., Hojo, J., and Okabe, Y. (1981). *Mem. Fac. Eng. Kyushi Univ.* 41:319.

Kinoshita, K., McLarnon, F. R., and Cairns, E. J. (1988). DOE Report DOE/METC-88/6096. U.S. Department of Energy-METC, Morgantown, p. 87.

Okuyama, K., Kousaka, Y., Tohge, N., Yamamoto, S., Wu, J. J., Flagan, R. C., and Seinfeld, J. H. (1986). *AIChE J.* 32:2010.

Scarlett, B., Merkus, H. G., Mori, Y., and Schoonman, J. (1988). In *Particle Size Analysis* (P. J. Lloyd, ed.). J. Wiley & Sons Ltd., New York, p. 107.

Singhal, S. C. (1991). In *Proceedings 1st International Symposium on SOFC's* (F. Grosz, P. Zegers, S. C. Singhal, and O. Yamamoto, eds.). Athens, July 2–5 1991. Commission of the European Communities, Luxembourg, p. 25.

Sipp, E., Langlais, F., and Naslain, R. (1992a). *J. Alloys Compounds* 186:65.

Sipp, E., Langlais, F., and Naslain, R. (1992b). *J. Alloys Compounds* 186:77.

Steele, B. C. H. (1990). In *Ceramics in Energy Applications: New Opportunities.* Proceedings, Institute of Energy Conference. Adam Hilger, Bristol, p. 173.

Strakhov, V. I., and Novikov, V. K. (1975). *J. Appl. Chem. USSR* 48:2819.

Received March 2, 1993; accepted June 15, 1993.